

Testing the $\Lambda(1520)$ hyperon in-medium width in near-threshold proton–nucleus reactions

E. Ya. Paryev

*Institute for Nuclear Research, Russian Academy of Sciences,
Moscow 117312, Russia*

Abstract

In the framework of the nuclear spectral function approach for incoherent primary proton–nucleon and secondary pion–nucleon production processes we study the inclusive $\Lambda(1520)$ hyperon production in the interaction of 2.83 GeV protons with nuclei. In particular, the A and momentum dependences of the absolute and relative $\Lambda(1520)$ hyperon yields are investigated in a two scenarios for its in-medium width. Our model calculations show that the pion–nucleon production channel contributes distinctly to the "low-momentum" $\Lambda(1520)$ creation both in light and heavy nuclei in the chosen kinematics and, hence, has to be taken into consideration on close examination of the dependences of the $\Lambda(1520)$ hyperon yields on the target mass number with the aim to get information on its width in the medium. They also demonstrate that both the A dependence of the relative $\Lambda(1520)$ hyperon production cross section and momentum dependence of the absolute $\Lambda(1520)$ hyperon yield at incident energy of interest are appreciably sensitive to the $\Lambda(1520)$ in-medium width, which means that these observables may be an important tool to determine the above width.

1. Introduction

The investigation of in-medium properties of hadrons (mainly light vector mesons ρ , ω , ϕ) produced in nuclei by heavy-ion and elementary-particle beams has received considerable interest in recent years (see, for example, [1]) in the context of observation of partial restoration of chiral symmetry—the fundamental symmetry of QCD in the limit of massless quarks—in the hot and dense nuclear matter. The another interesting case of resonance medium renormalization, recently found theoretically, is that of the $\Lambda(1520)$ hyperon where the hadronic model [2, 3] predicts appreciable medium effects in cold nuclear matter, e.g., an increase of the width of low-momentum $\Lambda(1520)$ hyperons at saturation density by a factor of five compared to its vacuum value ($\Gamma_{\Lambda(1520)} = 15.6$ MeV). Whereas the mass shift of the $\Lambda(1520)$ hyperon in nuclear matter is found to be small (about 2% of its free mass at normal nuclear matter density ρ_0) [2, 3]. The similar medium effects were predicted for the ϕ meson [4–7]. The possibility to learn about its total in-medium width has been considered in [8–15]. As a measure for the in-medium broadening of the ϕ meson the A dependence of its production cross section in nuclei in proton- and photon-induced reactions has been employed in these works. The A dependence is governed by the absorption of the ϕ meson flux in nuclear matter, which in turn is determined, in particular, by the phi in-medium width. Such method has been also recently adopted to study the properties of the ω in finite nuclei in γ -induced reactions [16–19].

Following the above method and using results of a model [2, 3] for the $\Lambda(1520)$ (or Λ^*) selfenergy in the nuclear medium as well as an eikonal approximation to account for the absorption of the outgoing $\Lambda(1520)$ resonance, the authors of [20] have calculated the A dependence of the ratio between the total $\Lambda(1520)$ production cross section in heavy nucleus and a light one (^{12}C) in γA and pA collisions. The calculations were performed within the local Fermi sea model at energies accessible at present experimental facilities like SPring-8, ELSA and COSY. They have been done also with considering only the relevant elementary one-step $\Lambda(1520)$ production mechanisms and thus with neglecting in part for pA reactions the $\Lambda(1520)$ creation in the two-step processes with an intermediate pions. These processes may contribute to the $\Lambda(1520)$ production in near-threshold pA interactions, much as the secondary pion-induced ϕ creation channels contribute [14, 15] to the ϕ production in such interactions. It is clear that, in order to get a deeper insight into the in-medium $\Lambda(1520)$ width in near-threshold pA reactions, it is necessary to clarify the relative role of the primary proton-nucleon and secondary pion-nucleon $\Lambda(1520)$ production processes in these reactions—the main purpose of the present investigation. Moreover, from the experimental point of view it is also important to evaluate not only the relative, but also the absolute $\Lambda(1520)$ production rates, which are lacking in [20], to elucidate the possibility of its real experimental observation in present facilities.

In this paper we perform a detailed analysis of the $\Lambda(1520)$ production in pA interactions at 2.83 GeV beam energy. This initial energy was used in the recent measurements of proton-induced ϕ production in nuclei at the ANKE-COSY facility [21]. We present the detailed predictions for the absolute and relative $\Lambda(1520)$ hyperon yields from these interactions obtained in the framework of a nuclear spectral function approach [14, 15] for an incoherent primary proton-nucleon ($pp \rightarrow pK^+\Lambda(1520)$, $pn \rightarrow nK^+\Lambda(1520)$, $pn \rightarrow pK^0\Lambda(1520)$) and secondary pion-nucleon ($\pi^+n \rightarrow K^+\Lambda(1520)$, $\pi^0p \rightarrow K^+\Lambda(1520)$, $\pi^0n \rightarrow K^0\Lambda(1520)$, $\pi^-p \rightarrow K^0\Lambda(1520)$) $\Lambda(1520)$ production processes in a two scenarios for its in-medium width. These predictions can be used as an important tool for possible extracting the valuable information on the $\Lambda(1520)$ in-medium width, for instance, from the data sample collected in the recent ANKE experiment [21] or from the data which could be taken in a devoted experiment at the CSR facility at Lanzhou (China).

2. The model and inputs

2.1. Direct $\Lambda(1520)$ production mechanism

An incident proton can produce a $\Lambda(1520)$ resonance directly in the first inelastic pN collision due to the nucleon's Fermi motion. Since we are interested in the near-threshold energy region, we have taken into account the following elementary processes which have the lowest free production threshold (≈ 2.77 GeV):

$$p + p \rightarrow p + K^+ + \Lambda(1520), \quad (1)$$

$$p + n \rightarrow n + K^+ + \Lambda(1520), \quad (2)$$

$$p + n \rightarrow p + K^0 + \Lambda(1520). \quad (3)$$

Because the $\Lambda(1520)N$ elastic scattering, similarly to the NN elastic collision, is expected to be sharply anisotropic at the relevant high (see below) $\Lambda(1520)$ laboratory momenta, we will neglect in the present study the loss of $\Lambda(1520)$ events in the given lab solid angle in the nuclear production due to the $\Lambda(1520)$ quasielastic rescatterings in the target nucleus. Moreover, since the $\Lambda(1520)$ hyperon pole mass in the medium is approximately not affected by medium effects [2, 3] as well as for reason of reducing the possible uncertainty of our calculations due to the use in them the model nucleon [22, 23] and kaon [23–25] selfenergies, we will also ignore the medium modification of the outgoing hadron masses in the present work. Then, taking into consideration the $\Lambda(1520)$ resonance final-state absorption as well as assuming that the $\Lambda(1520)$ hyperon—as a narrow resonance—is produced and propagated with its pole mass $M_{\Lambda(1520)}$ (or M_{Λ^*}) at small laboratory angles of our main interest ¹ and using the results given in [14, 15], we can represent the inclusive cross section for the production on nuclei $\Lambda(1520)$ hyperons with the momentum $\mathbf{p}_{\Lambda(1520)}$ (or \mathbf{p}_{Λ^*}) from the primary proton-induced reaction channels (1)–(3) as follows ² :

$$\frac{d\sigma_{pA \rightarrow \Lambda(1520)X}^{(\text{prim})}(\mathbf{p}_0)}{d\mathbf{p}_{\Lambda^*}} = I_V[A] \quad (4)$$

$$\times \left[\frac{Z}{A} \left\langle \frac{d\sigma_{pp \rightarrow pK^+\Lambda(1520)}(\mathbf{p}'_0, M_{\Lambda^*}, \mathbf{p}_{\Lambda^*})}{d\mathbf{p}_{\Lambda^*}} \right\rangle + 2 \frac{N}{A} \left\langle \frac{d\sigma_{pn \rightarrow nK^+\Lambda(1520)}(\mathbf{p}'_0, M_{\Lambda^*}, \mathbf{p}_{\Lambda^*})}{d\mathbf{p}_{\Lambda^*}} \right\rangle \right],$$

where

$$I_V[A] = 2\pi A \int_0^R r_{\perp} dr_{\perp} \int_{-\sqrt{R^2-r_{\perp}^2}}^{\sqrt{R^2-r_{\perp}^2}} dz \rho(\sqrt{r_{\perp}^2+z^2}) \quad (5)$$

$$\times \exp \left[-\sigma_{pN}^{\text{in}} A \int_{-\sqrt{R^2-r_{\perp}^2}}^z \rho(\sqrt{r_{\perp}^2+x^2}) dx - \int_z^{\sqrt{R^2-r_{\perp}^2}} \frac{dx}{\lambda_{\Lambda^*}(\sqrt{r_{\perp}^2+x^2}, M_{\Lambda^*})} \right],$$

$$\lambda_{\Lambda^*}(\mathbf{r}, M_{\Lambda^*}) = \frac{p_{\Lambda^*}}{M_{\Lambda^*} \Gamma_{\text{tot}}(\mathbf{r}, M_{\Lambda^*})} \quad (6)$$

¹A choice of these angles has been motivated by the fact that in the threshold energy region $\Lambda(1520)$ hyperons are mainly emitted in forward directions.

²It is worth noting that for kinematical conditions of our interest the contribution to the $\Lambda(1520)$ production on nuclei from the $\Lambda(1520)$ hyperons produced in primary $pN \rightarrow NK\Lambda(1520)$ channels (1)–(3) and decaying into the K^-p pairs (whereby the $\Lambda(1520)$ can be detected, for example, by the ANKE spectrometer) inside the target nucleus is found on the basis of the model developed in [26] to be negligible compared to the overall $\Lambda(1520)$ yield from primary and secondary $\Lambda(1520)$ creation processes calculated for these conditions within the present approach. The latter yield corresponds to the $\Lambda(1520)$ decays outside the target nucleus.

and

$$\left\langle \frac{d\sigma_{pN \rightarrow NK+\Lambda(1520)}(\mathbf{p}_0', M_{\Lambda^*}, \mathbf{p}_{\Lambda^*})}{d\mathbf{p}_{\Lambda^*}} \right\rangle = \int \int P(\mathbf{p}_t, E) d\mathbf{p}_t dE \left[\frac{d\sigma_{pN \rightarrow NK+\Lambda(1520)}(\sqrt{s}, M_{\Lambda^*}, \mathbf{p}_{\Lambda^*})}{d\mathbf{p}_{\Lambda^*}} \right], \quad (7)$$

$$s = (E_0' + E_t)^2 - (\mathbf{p}_0' + \mathbf{p}_t)^2, \quad (8)$$

$$E_0' = E_0 - \frac{\Delta \mathbf{p}^2}{2M_A}, \quad (9)$$

$$\mathbf{p}_0' = \mathbf{p}_0 - \Delta \mathbf{p}, \quad (10)$$

$$\Delta \mathbf{p} = \frac{E_0 V_0}{p_0} \frac{\mathbf{p}_0}{|\mathbf{p}_0|}, \quad (11)$$

$$E_t = M_A - \sqrt{(-\mathbf{p}_t)^2 + (M_A - m_N + E)^2}. \quad (12)$$

Here, $d\sigma_{pN \rightarrow NK+\Lambda(1520)}(\sqrt{s}, M_{\Lambda^*}, \mathbf{p}_{\Lambda^*})/d\mathbf{p}_{\Lambda^*}$ are the off-shell differential cross sections for $\Lambda(1520)$ production in reactions (1) and (2) at the pN center-of-mass energy \sqrt{s} ; $\rho(\mathbf{r})$ and $P(\mathbf{p}_t, E)$ are the nucleon density and nuclear spectral function normalized to unity; \mathbf{p}_t and E are the internal momentum and removal energy of the struck target nucleon just before the collision; σ_{pN}^{in} and $\Gamma_{\text{tot}}(\mathbf{r}, M_{\Lambda^*})$ are the inelastic cross section³ of free pN interaction and total $\Lambda(1520)$ width in its rest frame, taken at the point \mathbf{r} inside the nucleus and at the pole of the resonance; Z and N are the numbers of protons and neutrons in the target nucleus ($A = N + Z$), M_A and R are its mass and radius; m_N is the bare nucleon mass; \mathbf{p}_0 and E_0 are the momentum and total energy of the initial proton; V_0 is the nuclear optical potential that this proton feels in the interior of the nucleus ($V_0 \approx 40$ MeV). When obtaining eq. (4) we used the fact that the $\Lambda(1520)$ hyperon production cross sections in reactions (2) and (3) are the same due to the isospin symmetry. The first term in it describes the contribution to the $\Lambda(1520)$ resonance production on nuclei from the primary pp interaction (1), whereas the second one represents the contribution to this production from the pn elementary processes (2) and (3). The quantity $I_V[A]$ in eq. (4) represents the effective number of target nucleons participating in the primary $pN \rightarrow NK\Lambda(1520)$ reactions. It is calculated according to equation (5) in which the first and the second exponential factors describe, respectively, the distortion of the initial proton inside the nucleus till the reaction point as well as the attenuation of the outgoing $\Lambda(1520)$ hyperon in its way out of the nucleus.

Let us now specify the off-shell differential cross sections $d\sigma_{pN \rightarrow NK+\Lambda(1520)}(\sqrt{s}, M_{\Lambda^*}, \mathbf{p}_{\Lambda^*})/d\mathbf{p}_{\Lambda^*}$ for $\Lambda(1520)$ production in the reactions (1), (2), entering into eqs. (4), (7). Following refs. [14, 15, 26–28], we assume that these cross sections are equivalent to the respective on-shell cross sections calculated for the off-shell kinematics of the elementary processes (1), (2). In our approach the differential cross sections for $\Lambda(1520)$ production in the reactions (1), (2) have been described by the three-body phase space calculations normalized to the corresponding total cross sections $\sigma_{pN \rightarrow NK+\Lambda(1520)}(\sqrt{s})$ [14, 15]:

$$\frac{d\sigma_{pN \rightarrow NK+\Lambda(1520)}(\sqrt{s}, M_{\Lambda^*}, \mathbf{p}_{\Lambda^*})}{d\mathbf{p}_{\Lambda^*}} = \frac{\pi}{4E_{\Lambda^*}} \frac{\sigma_{pN \rightarrow NK+\Lambda(1520)}(\sqrt{s})}{I_3(s, m_N, m_K, M_{\Lambda^*})} \frac{\lambda(s_{NK}, m_N^2, m_K^2)}{s_{NK}}, \quad (13)$$

$$I_3(s, m_N, m_K, M_{\Lambda^*}) = \left(\frac{\pi}{2}\right)^2 \int_{(m_N+m_K)^2}^{(\sqrt{s}-M_{\Lambda^*})^2} \frac{\lambda(s_{NK}, m_N^2, m_K^2)}{s_{NK}} \frac{\lambda(s, s_{NK}, M_{\Lambda^*}^2)}{s} ds_{NK}, \quad (14)$$

$$\lambda(x, y, z) = \sqrt{[x - (\sqrt{y} + \sqrt{z})^2][x - (\sqrt{y} - \sqrt{z})^2]}, \quad (15)$$

³We use $\sigma_{pN}^{\text{in}} = 30$ mb for considered projectile proton energy of $\epsilon_0 = 2.83$ GeV [14].

$$s_{NK} = s + M_{\Lambda^*}^2 - 2(E_0' + E_t)E_{\Lambda^*} + 2(\mathbf{p}_0' + \mathbf{p}_t)\mathbf{p}_{\Lambda^*}. \quad (16)$$

Here, E_{Λ^*} is the total energy of a $\Lambda(1520)$ hyperon ($E_{\Lambda^*} = \sqrt{p_{\Lambda^*}^2 + M_{\Lambda^*}^2}$) and m_K is the bare kaon mass.

Up to now, there have been no data on $\Lambda(1520)$ production in reactions (1) and (2). There is [29] only one data point $(6.09 \pm 1.74) \mu\text{b}$ for the free total cross section $\sigma_{pn \rightarrow pK^0\Lambda(1520)}(\sqrt{s})$ of the reaction (3) at 0.8 GeV excess energy ⁴ (or at beam momentum of 6.5 GeV/c). To estimate the $pN \rightarrow NK^+\Lambda(1520)$ free total cross sections $\sigma_{pN \rightarrow NK^+\Lambda(1520)}(\sqrt{s})$, entering into eq. (13), we have employed the one-pion-exchange model [30–32]. This model reasonably reproduces the available experimental data from many nucleon–nucleon collision processes in a few GeV energy region. The one-pion-exchange diagram, for example, for the reaction $pp \rightarrow pK^+\Lambda(1520)$ is shown in figure 1. Assuming the on-shell approximation for the virtual process $\pi^0 p \rightarrow K^+\Lambda(1520)$, the total cross

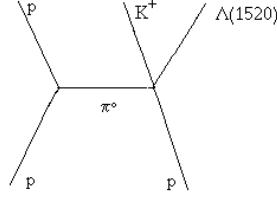


Figure 1: Diagram representing process (1).

section for this reaction at the center-of-mass energy \sqrt{s} can be written as [30–32]:

$$\sigma_{pp \rightarrow pK^+\Lambda(1520)}(\sqrt{s}) = 2\sigma_A(\sqrt{s}), \quad (17)$$

$$\sigma_A(\sqrt{s}) = \frac{1}{(2\pi)^2 (p_0^* \sqrt{s})^2} \frac{m_p^2}{m_\pi^2} f_{\pi NN}^2 \quad (18)$$

$$\times \int_{(m_K + M_{\Lambda^*})}^{(\sqrt{s} - m_p)} k s_1 d(\sqrt{s_1}) \sigma_{\pi^0 p \rightarrow K^+\Lambda(1520)}(\sqrt{s_1}) \int_{t_-}^{t_+} (-t) dt D^2(t) F^2(t),$$

where

$$k = \frac{1}{2\sqrt{s_1}} \lambda(s_1, m_p^2, m_\pi^2), \quad (19)$$

$$t_\pm = 2m_p^2 - 2E_0^* E_f^* \pm 2p_0^* p_f^*, \quad (20)$$

$$p_0^* = \frac{1}{2\sqrt{s}} \lambda(s, m_p^2, m_p^2), \quad p_f^* = \frac{1}{2\sqrt{s}} \lambda(s, s_1, m_p^2), \quad (21)$$

$$E_0^* = \sqrt{p_0^{*2} + m_p^2}, \quad E_f^* = \sqrt{p_f^{*2} + m_p^2} \quad (22)$$

and

$$D(t) = \frac{1}{t - m_\pi^2}, \quad (23)$$

⁴Which is defined as $\sqrt{s} - \sqrt{s_{th}}$, where $\sqrt{s_{th}} = m_p + m_K + M_{\Lambda^*}$ is the threshold energy.

$$F(t) = \frac{\Lambda_\pi^2 - m_\pi^2}{\Lambda_\pi^2 - t}. \quad (24)$$

Here, m_π is the pion mass, Λ_π is the respective cut-off parameter, $f_{\pi NN}$ is the coupling constant⁵, and $\sigma_{\pi^0 p \rightarrow K^+ \Lambda(1520)}(\sqrt{s_1})$ is the on-shell total cross section for the reaction $\pi^0 p \rightarrow K^+ \Lambda(1520)$ at the πN center-of-mass energy $\sqrt{s_1}$. The quantity λ , entering into eqs. (19) and (21), is defined above by the formula (15). According to the isospin considerations, we have:

$$\sigma_{\pi^0 p \rightarrow K^+ \Lambda(1520)} = \frac{1}{2} \sigma_{\pi^- p \rightarrow K^0 \Lambda(1520)}. \quad (25)$$

For the free total cross section $\sigma_{\pi^- p \rightarrow K^0 \Lambda(1520)}$ we have used the following parametrization:

$$\sigma_{\pi^- p \rightarrow K^0 \Lambda(1520)}(\sqrt{s_1}) = \begin{cases} 123 (\sqrt{s_1} - \sqrt{s_0})^{0.47} [\mu\text{b}] & \text{for } 0 < \sqrt{s_1} - \sqrt{s_0} \leq 0.427 \text{ GeV}, \\ 26.6 / (\sqrt{s_1} - \sqrt{s_0})^{1.33} [\mu\text{b}] & \text{for } \sqrt{s_1} - \sqrt{s_0} > 0.427 \text{ GeV}, \end{cases} \quad (26)$$

where $\sqrt{s_0} = 2.017$ GeV is the threshold energy for $\pi^- p \rightarrow K^0 \Lambda(1520)$ reaction. The comparison of the results of our calculations by (26) (solid line) with the available experimental data (full squares) [33] for this reaction is shown in figure 2. It is seen that our parametrization (26) fits well the

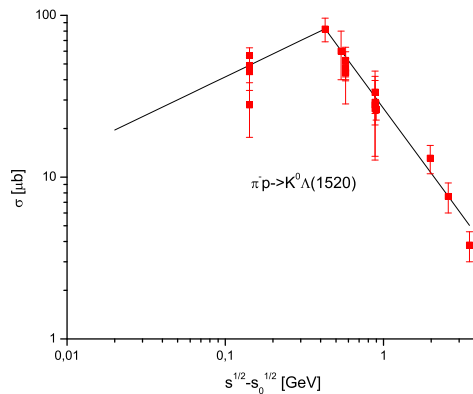


Figure 2: Total cross section for $\Lambda(1520)$ production in the reaction $\pi^- p \rightarrow K^0 \Lambda(1520)$ as a function of excess energy $\sqrt{s} - \sqrt{s_0}$. For notation see the text.

existing set of data for the $\pi^- p \rightarrow K^0 \Lambda(1520)$ reaction. For the cut-off parameter Λ_π , entering into eq. (24), we use $\Lambda_\pi = 0.7$ GeV in order to describe (see figure 3) by means of the relation

$$\sigma_{pn \rightarrow pK^0 \Lambda(1520)} = 2.5 \sigma_{pp \rightarrow pK^+ \Lambda(1520)}, \quad (27)$$

which the one-pion-exchange model of [30–32] gives, and eqs. (17)–(26) the $pn \rightarrow pK^0 \Lambda(1520)$ data point at 0.8 GeV excess energy mentioned above. In figure 3 we show also the calculated cross section of the reaction $pp \rightarrow pK^+ \Lambda(1520)$, for which there are presently no experimental data. Looking at this figure and keeping in mind that $\sigma_{pn \rightarrow nK^+ \Lambda(1520)} = \sigma_{pn \rightarrow pK^0 \Lambda(1520)}$ due to the isospin symmetry, one can see that for the incoming proton energy of 2.83 GeV of our interest (which corresponds to the excess energy of 20 MeV) the value of the total $\Lambda(1520)$ hyperon production cross section in proton–proton and proton–neutron collisions is of the order of 2 and 10 nb, respectively. The latter values are very small, but one should expect to measure theirs on ANKE-at-COSY facility [34] in order to check the results of our model calculations of the primary elementary total cross

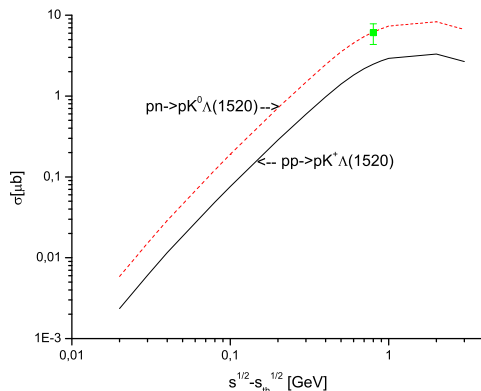


Figure 3: Total cross sections for the reactions $pp \rightarrow pK^+\Lambda(1520)$ (solid line) and $pn \rightarrow pK^0\Lambda(1520)$ (dotted line) as functions of excess energy $\sqrt{s} - \sqrt{s_{th}}$ calculated, respectively, by (17)–(26) and (17)–(27) with $\Lambda_\pi = 0.7$ GeV. The experimental data point for the $pn \rightarrow pK^0\Lambda(1520)$ process is taken from [29].

sections, which will be used below to calculate the yield of $\Lambda(1520)$ hyperons from proton–nucleus interactions.

For the $\Lambda(1520)$ production calculations in the case of ^{12}C and ^{27}Al , ^{63}Cu , ^{108}Ag , ^{197}Au , ^{238}U target nuclei reported here we have employed for the nuclear density $\rho(\mathbf{r})$, respectively, the harmonic oscillator and the Woods-Saxon distributions, given in [14]. The nuclear spectral function $P(\mathbf{p}_t, E)$ (which represents the probability to find a nucleon with momentum \mathbf{p}_t and removal energy E in the nucleus) for these target nuclei was taken from [14, 15, 35–38].

Let us concentrate now on the total $\Lambda(1520)$ in-medium width appearing in (6) and used in the subsequent calculations of $\Lambda(1520)$ resonance attenuation in pA interactions.

For this width we adopt two different scenarios: **i)** no in-medium effects and, correspondingly, the scenario with the free $\Lambda(1520)$ width ⁶ (dotted line in figure 4); **ii)** the sum of the free $\Lambda(1520)$ width and its collisional width of the type [2, 3, 20] $55(\rho_N/\rho_0)$ MeV, where ρ_N is the nucleon density (solid line ⁷ in figure 4). According to [2, 3], the above collisional width is mainly governed by the following $\Lambda(1520)N$ interactions: $\Lambda(1520)N \rightarrow N\Lambda(1116)$, $\Lambda(1520)N \rightarrow N\Sigma(1189)$, $\Lambda(1520)N \rightarrow N\Sigma(1385)$, $\Lambda(1520)N \rightarrow \Delta\Sigma(1189)$, $\Lambda(1520)N \rightarrow \Delta\Sigma(1385)$. Therefore, the study of the $\Lambda(1520)$ absorption in nuclear medium can help using the low-density approximation [1] to determine the unknown $\Lambda(1520)N$ inelastic cross section. It should be noted that the adoption of the $\Lambda(1520)$ in-medium width, depicted by solid line in figure 4, is justified only for small $\Lambda(1520)$ laboratory momenta [2, 3]. For high $\Lambda(1520)$ momenta it is needed, strictly speaking, to account for in the calculations the momentum dependence of this width which emerges in particular from the (moderate) momentum dependence of the imaginary part, $Im\Sigma_{\Lambda^*}$, of the $\Lambda(1520)$ selfenergy in nuclear matter found in

⁵Which was taken in the calculations to be equal to 1.0 [31, 32].

⁶Experimentally, the $\Lambda(1520)$ hyperons can be detected (for example, by the ANKE spectrometer) from their $\Lambda(1520) \rightarrow K^-p$ decay channel, having branching ratio $\approx 23\%$. The $\Lambda(1520)$ decays $\Lambda(1520) \rightarrow \bar{K}^0n$, $\Sigma\pi$, $\Lambda_2\pi$, which exhaust $\approx 75\%$ of its free width, do not go into this detection channel and hence lead to the loss (or absorption) of $\Lambda(1520)$ flux inside the nucleus with respect to this channel. Due to the strong final-state interactions of the K^- and p decay products, it does not contribute practically to the $\Lambda(1520)$ production on nuclei (cf. footnote 2). All the above means, that the free $\Lambda(1520)$ width induces a reduction of the number of the detectable $\Lambda(1520)$ hyperons and should be taken into account in the calculation of $\Lambda(1520)$ production on nuclei.

⁷It shows that in this scenario the resulting total (decay + collisional) width of the $\Lambda(1520)$ hyperon grows as a function of the density and reaches the value of around 70 MeV at the density ρ_0 , which by a factor of ~ 5 bigger than the free one.

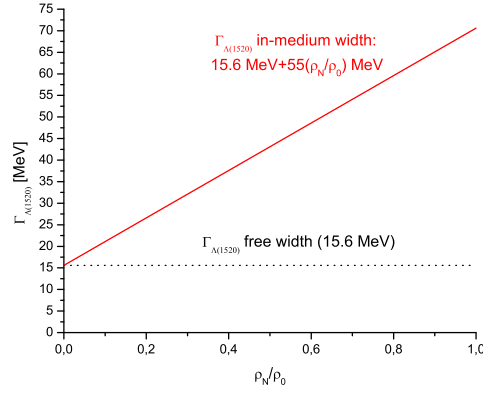


Figure 4: $\Lambda(1520)$ hyperon total width as a function of density. For notation see the text.

[3] through the relation [20]: $\Gamma_{\text{tot}} = -(2E_{\Lambda^*} \text{Im}\Sigma_{\Lambda^*})/M_{\Lambda^*}$. However, because the main goal of the present study was to clarify the role of the secondary pion–nucleon $\Lambda(1520)$ production process in near-threshold pA reactions as well as for the sake of numerical simplicity, we neglect the momentum dependence of the in-medium $\Lambda(1520)$ width Γ_{tot} in our calculations. Evidently, this enables us to obtain an upper estimate of the strength of the respective double differential cross sections and leads to the enlarged A dependence of the ratio between the $\Lambda(1520)$ production cross section in heavy nucleus and a light one especially in the region of heavy target nuclei where the absorption effect is strong (see below).

Let us consider now the two-step $\Lambda(1520)$ production mechanism.

2.2. Two-step $\Lambda(1520)$ production mechanism

At the bombarding energy of our interest (2.83 GeV) the following two-step $\Lambda(1520)$ production process with a pion in an intermediate state may contribute to the $\Lambda(1520)$ creation in pA interactions:

$$p + N_1 \rightarrow \pi + X, \quad (28)$$

$$\pi + N_2 \rightarrow K + \Lambda(1520), \quad (29)$$

provided that the latter subprocess is allowed energetically⁸. Here, K stands for K^+ or K^0 for the specific isospin channel. Taking into account the $\Lambda(1520)$ final-state absorption and ignoring the influence⁹ of the nuclear environment on the outgoing hadron masses in the $\Lambda(1520)$ production channel (29) as well as using the results given in [14, 15], we get the following expression for the $\Lambda(1520)$ production cross section for pA reactions at small laboratory angles of interest from this channel:

$$\frac{d\sigma_{pA \rightarrow \Lambda(1520)X}^{(\text{sec})}(\mathbf{p}_0)}{d\mathbf{p}_{\Lambda^*}} = \frac{I_V^{(\text{sec})}[A]}{I_V'[A]} \sum_{\pi=\pi^+, \pi^0, \pi^-} \int_{4\pi} d\Omega_{\pi} \int_{p_{\pi}^{\text{abs}}}^{p_{\pi}^{\text{lim}}(\vartheta_{\pi})} p_{\pi}^2 dp_{\pi} \frac{d\sigma_{pA \rightarrow \pi X}^{(\text{prim})}(\mathbf{p}_0)}{d\mathbf{p}_{\pi}} \times \quad (30)$$

$$\times \left[\frac{Z}{A} \left\langle \frac{d\sigma_{\pi p \rightarrow K\Lambda(1520)}(\mathbf{p}_{\pi}, \mathbf{p}_{\Lambda^*})}{d\mathbf{p}_{\Lambda^*}} \right\rangle + \frac{N}{A} \left\langle \frac{d\sigma_{\pi n \rightarrow K\Lambda(1520)}(\mathbf{p}_{\pi}, \mathbf{p}_{\Lambda^*})}{d\mathbf{p}_{\Lambda^*}} \right\rangle \right],$$

⁸We remind that the free threshold energy for this subprocess amounts to 1.55 GeV.

⁹In line with the assumption about the absence of such influence on the final hadron masses in primary proton-induced reaction channels (1)–(3).

where

$$I_V^{(\text{sec})}[A] = 2\pi A^2 \int_0^R r_\perp dr_\perp \int_{-\sqrt{R^2-r_\perp^2}}^{\sqrt{R^2-r_\perp^2}} dz \rho(\sqrt{r_\perp^2+z^2}) \int_0^{\sqrt{R^2-r_\perp^2}-z} dl \rho(\sqrt{r_\perp^2+(z+l)^2}) \times \quad (31)$$

$$\times \exp \left[-\sigma_{pN}^{\text{in}} A \int_{-\sqrt{R^2-r_\perp^2}}^z \rho(\sqrt{r_\perp^2+x^2}) dx - \sigma_{\pi N}^{\text{tot}} A \int_z^{z+l} \rho(\sqrt{r_\perp^2+x^2}) dx \right] \times$$

$$\times \exp \left[- \int_{z+l}^{\sqrt{R^2-r_\perp^2}} \frac{dx}{\lambda_{\Lambda^*}(\sqrt{r_\perp^2+x^2}, M_{\Lambda^*})} \right],$$

$$I_V'[A] = 2\pi A \int_0^R r_\perp dr_\perp \int_{-\sqrt{R^2-r_\perp^2}}^{\sqrt{R^2-r_\perp^2}} dz \rho(\sqrt{r_\perp^2+z^2}) \times \quad (32)$$

$$\times \exp \left[-\sigma_{pN}^{\text{in}} A \int_{-\sqrt{R^2-r_\perp^2}}^z \rho(\sqrt{r_\perp^2+x^2}) dx - \sigma_{\pi N}^{\text{tot}} A \int_z^{\sqrt{R^2-r_\perp^2}} \rho(\sqrt{r_\perp^2+x^2}) dx \right],$$

$$\left\langle \frac{d\sigma_{\pi N \rightarrow K\Lambda(1520)}(\mathbf{p}_\pi, \mathbf{p}_{\Lambda^*})}{d\mathbf{p}_{\Lambda^*}} \right\rangle = \int \int P(\mathbf{p}_t, E) d\mathbf{p}_t dE \left[\frac{d\sigma_{\pi N \rightarrow K\Lambda(1520)}(\sqrt{s_1}, \mathbf{p}_{\Lambda^*})}{d\mathbf{p}_{\Lambda^*}} \right]; \quad (33)$$

$$s_1 = (E_\pi + E_t)^2 - (p_\pi \boldsymbol{\Omega}_0 + \mathbf{p}_t)^2, \quad (34)$$

$$p_\pi^{\text{lim}}(\vartheta_\pi) = \frac{\beta_A p_0 \cos \vartheta_\pi + (E_0 + M_A) \sqrt{\beta_A^2 - 4m_\pi^2 (s_A + p_0^2 \sin^2 \vartheta_\pi)}}{2(s_A + p_0^2 \sin^2 \vartheta_\pi)}, \quad (35)$$

$$\beta_A = s_A + m_\pi^2 - M_{A+1}^2, \quad s_A = (E_0 + M_A)^2 - p_0^2, \quad (36)$$

$$\cos \vartheta_\pi = \boldsymbol{\Omega}_0 \boldsymbol{\Omega}_\pi, \quad \boldsymbol{\Omega}_0 = \mathbf{p}_0/p_0, \quad \boldsymbol{\Omega}_\pi = \mathbf{p}_\pi/p_\pi. \quad (37)$$

Here, $d\sigma_{pA \rightarrow \pi X}^{(\text{prim})}(\mathbf{p}_0)/d\mathbf{p}_\pi$ are the inclusive differential cross sections for pion production on nuclei at small laboratory angles and for high momenta from the primary proton-induced reaction channel (28); $d\sigma_{\pi N \rightarrow K\Lambda(1520)}(\sqrt{s_1}, \mathbf{p}_{\Lambda^*})/d\mathbf{p}_{\Lambda^*}$ is the free inclusive differential cross section for $\Lambda(1520)$ production via the subprocess (29) calculated for the off-shell kinematics of this subprocess at the πN center-of-mass energy $\sqrt{s_1}$; $\sigma_{\pi N}^{\text{tot}}$ is the total cross section of the free πN interaction¹⁰; \mathbf{p}_π and E_π are the momentum and total energy of a pion (which is assumed to be on-shell); p_π^{abs} is the absolute threshold momentum for $\Lambda(1520)$ production on the residual nucleus by an intermediate pion; $p_\pi^{\text{lim}}(\vartheta_\pi)$ is the kinematical limit for pion production at the lab angle ϑ_π from proton-nucleus collisions. The quantity λ_{Λ^*} is defined above by eq. (6). As is seen from eq. (30), we evaluate the $\Lambda(1520)$ yield for pA reactions from the secondary process (29) by folding the respective pion distribution from the primary proton-induced reaction channel (28) (denoted by¹¹ $[d\sigma_{pA \rightarrow \pi X}^{(\text{prim})}(\mathbf{p}_0)/d\mathbf{p}_\pi]/I_V'[A]$) with the momentum-removal energy-averaged inclusive differential cross section for $\Lambda(1520)$ production in this process (denoted by $\langle d\sigma_{\pi N \rightarrow K\Lambda(1520)}(\mathbf{p}_\pi, \mathbf{p}_{\Lambda^*})/d\mathbf{p}_{\Lambda^*} \rangle$) and with the effective number of $N_1 N_2$ pairs per unit of area (denoted via $I_V^{(\text{sec})}[A]$), involved in the two-step $\Lambda(1520)$ production chain under consideration. In the expression (31), which defines the quantity $I_V^{(\text{sec})}[A]$, the first two

¹⁰We use in the following calculations $\sigma_{\pi N}^{\text{tot}} = 35$ mb for all pion momenta [14, 15].

¹¹Where $I_V'[A]$ is the effective number of target nucleons participating in this channel (see eq. (32)).

eikonal factors account for the distortion of the incident proton and intermediate pion inside the target nucleus, whereas the latter one describes the attenuation of the produced $\Lambda(1520)$ hyperon in its way out of the nucleus.

The expression for the differential cross section for $\Lambda(1520)$ production in the elementary process (29) has the following form:

$$\frac{d\sigma_{\pi N \rightarrow K\Lambda(1520)}(\sqrt{s_1}, \mathbf{p}_{\Lambda^*})}{d\mathbf{p}_{\Lambda^*}} = \frac{\pi}{I_2(s_1, m_K, M_{\Lambda^*})E_{\Lambda^*}} \frac{d\sigma_{\pi N \rightarrow K\Lambda(1520)}(\sqrt{s_1})}{d\Omega_{\Lambda^*}^*} \times \quad (38)$$

$$\times \frac{1}{(\omega + E_t)} \delta \left[\omega + E_t - \sqrt{m_K^2 + (\mathbf{Q} + \mathbf{p}_t)^2} \right],$$

where

$$I_2(s_1, m_K, M_{\Lambda^*}) = \frac{\pi \lambda(s_1, m_K^2, M_{\Lambda^*}^2)}{2 s_1}, \quad (39)$$

$$\omega = E_\pi - E_{\Lambda^*}, \quad \mathbf{Q} = \mathbf{p}_\pi - \mathbf{p}_{\Lambda^*}. \quad (40)$$

In eq. (38), $d\sigma_{\pi N \rightarrow K\Lambda(1520)}(\sqrt{s_1})/d\Omega_{\Lambda^*}^*$ is the differential cross section for $\Lambda(1520)$ production in reaction (29) in the πN c.m.s., which is assumed to be isotropic in our calculations of $\Lambda(1520)$ creation in pA collisions from this reaction:

$$\frac{d\sigma_{\pi N \rightarrow K\Lambda(1520)}(\sqrt{s_1})}{d\Omega_{\Lambda^*}^*} = \frac{\sigma_{\pi N \rightarrow K\Lambda(1520)}(\sqrt{s_1})}{4\pi}. \quad (41)$$

Here, $\sigma_{\pi N \rightarrow K\Lambda(1520)}(\sqrt{s_1})$ is the total cross section of the elementary process $\pi N \rightarrow K\Lambda(1520)$. The elementary $\Lambda(1520)$ production reactions $\pi^+ n \rightarrow K^+ \Lambda(1520)$, $\pi^0 p \rightarrow K^+ \Lambda(1520)$, $\pi^0 n \rightarrow K^0 \Lambda(1520)$ and $\pi^- p \rightarrow K^0 \Lambda(1520)$ have been included in our calculations of the $\Lambda(1520)$ production on nuclei. The isospin considerations show that the following relations among the total cross sections of these reactions exist:

$$\sigma_{\pi^+ n \rightarrow K^+ \Lambda(1520)} = \sigma_{\pi^- p \rightarrow K^0 \Lambda(1520)}, \quad (42)$$

$$\sigma_{\pi^0 p \rightarrow K^+ \Lambda(1520)} = \sigma_{\pi^0 n \rightarrow K^0 \Lambda(1520)} = \frac{1}{2} \sigma_{\pi^- p \rightarrow K^0 \Lambda(1520)}. \quad (43)$$

For the free total cross section $\sigma_{\pi^- p \rightarrow K^0 \Lambda(1520)}$ we have used the suggested above parametrization (26).

Another very important ingredient for the calculation of the $\Lambda(1520)$ production cross section in proton–nucleus reactions from pion-induced reaction channel (29)—the high-momentum parts of the differential cross sections for pion production on nuclei at small lab angles from the primary process (28) was taken from [14, 15, 37, 38].

Now, let us proceed to the discussion of the results of our calculations for $\Lambda(1520)$ production in pA interactions in the framework of the model outlined above.

3. Results and discussion

At first, we consider the absolute $\Lambda(1520)$ production cross sections from the one-step and two-step $\Lambda(1520)$ creation mechanisms in $p^{12}\text{C}$, $p^{63}\text{Cu}$, $p^{197}\text{Au}$ collisions calculated on the basis of eqs. (4), (30) for proton kinetic energy of 2.83 GeV and for the laboratory $\Lambda(1520)$ production angle of 0° in two considered scenarios (see figure 4) for the total $\Lambda(1520)$ in-medium width. The cross sections calculated using the free $\Lambda(1520)$ width for this width are depicted in figure 5. Whereas the ones obtained for in-medium $\Lambda(1520)$ width shown by solid curve in figure 4 are given in figure 6. Looking at these figures, one can see that the primary $pN \rightarrow NK\Lambda(1520)$ processes play the dominant role at $\Lambda(1520)$ momenta ≥ 1.7 GeV/c for all considered target nuclei and for both adopted

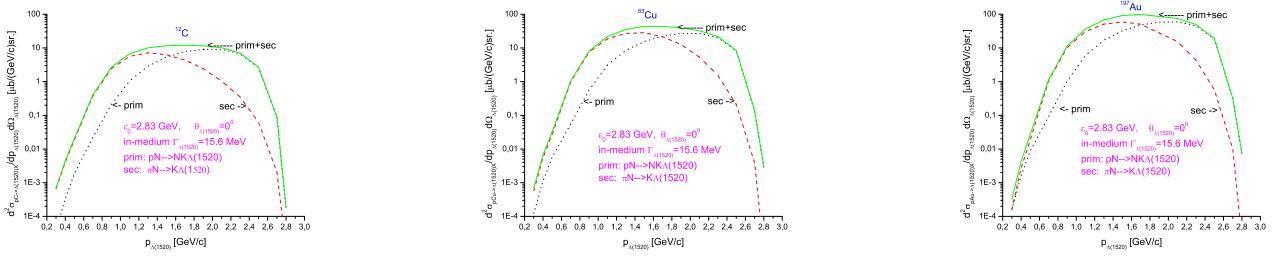


Figure 5: Double differential cross sections for the production of $\Lambda(1520)$ hyperons at a lab angle of 0° in the interaction of protons of energy 2.83 GeV with ^{12}C (left panel), ^{63}Cu (middle panel) and ^{197}Au (right panel) nuclei as functions of $\Lambda(1520)$ momentum. The dotted and dashed lines are calculations, respectively, for the one- and two-step $\Lambda(1520)$ creation mechanisms. The solid line is the sum of the dotted and dashed lines. The loss of $\Lambda(1520)$ hyperons in nuclear matter was determined by their free width (dotted curve in figure 4).

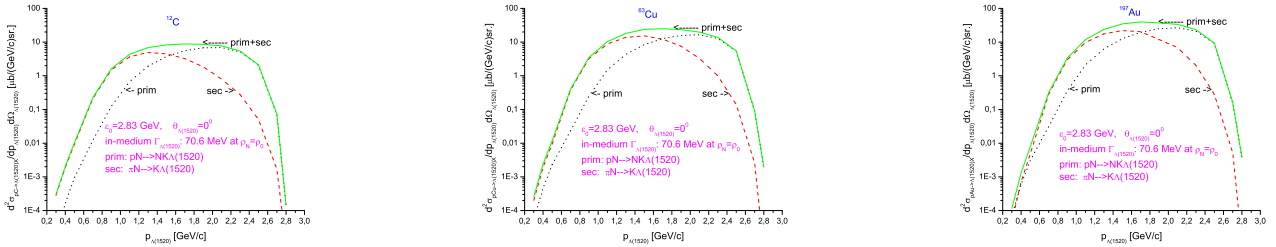


Figure 6: Double differential cross sections for the production of $\Lambda(1520)$ hyperons at a lab angle of 0° in the interaction of protons of energy 2.83 GeV with ^{12}C (left panel), ^{63}Cu (middle panel) and ^{197}Au (right panel) nuclei as functions of $\Lambda(1520)$ momentum. The dotted and dashed lines are calculations, respectively, for the one- and two-step $\Lambda(1520)$ creation mechanisms. The solid line is the sum of the dotted and dashed lines. The absorption of $\Lambda(1520)$ hyperons in nuclear matter was governed by their in-medium width shown by solid curve in figure 4.

scenarios for the $\Lambda(1520)$ in-medium width, whereas at lower $\Lambda(1520)$ momenta the secondary pion-induced reaction channel $\pi N \rightarrow K\Lambda(1520)$ is clearly dominant only for ^{12}C and ^{63}Cu target nuclei. In the case of having ^{197}Au as target nucleus, this channel dominates the $\Lambda(1520)$ production only at $\Lambda(1520)$ momenta $0.5 \text{ GeV}/c \leq p_{\Lambda(1520)} \leq 1.7 \text{ GeV}/c$, whereas at $\Lambda(1520)$ momenta $\leq 0.5 \text{ GeV}/c$ its dominance, contrary to the results for ^{12}C and ^{63}Cu , is less pronounced. This means that the channel $\pi N \rightarrow K\Lambda(1520)$ has to be taken into consideration on close examination¹² of the A dependence of the relative $\Lambda(1520)$ hyperon production cross section in proton–nucleus reactions at energies just above threshold with the aim of extracting of the information on the $\Lambda(1520)$ width in nuclear medium. Comparing the results of our full calculations (the sum of contributions both from primary and from secondary $\Lambda(1520)$ production processes) presented in figures 5 and 6 by solid lines, we see yet that for given target nucleus there is clear difference between the results obtained by using different $\Lambda(1520)$ in-medium widths under consideration. We may see, for example, that for the considered ^{12}C , ^{63}Cu and ^{197}Au nuclei the cross section in the momentum range $\sim 1.2\text{--}2.4 \text{ GeV}/c$ (where it is the greatest) when calculated with the increased $\Lambda(1520)$ width in the medium is reduced, respectively, by a factors of about 1.3, 1.6 and 2.3 compared to that obtained in the case when the loss of $\Lambda(1520)$ hyperons in nuclear matter was determined by their free width.

In figure 7 we show together the results of our overall calculations, given before separately in

¹²In particular, of the A dependence of the ratio between the total $\Lambda(1520)$ production cross section in heavy nucleus and a light one in pA collisions. Let us remind that the latter observable has been studied in [20] without accounting for the process $\pi N \rightarrow K\Lambda(1520)$.

figures 5 and 6 by solid lines, for the double differential cross sections for the production of $\Lambda(1520)$ hyperons on ^{12}C and ^{197}Au target nuclei at a lab angle of 0° for the primary (1)–(3) plus secondary (29) $\Lambda(1520)$ creation processes obtained for bombarding energy of 2.83 GeV by employing in them both the free $\Lambda(1520)$ hyperons width (dotted lines) and their in-medium width shown by solid curve in figure 4 (solid lines) to see more clearly the sensitivity of the calculated cross sections to the choice of the $\Lambda(1520)$ in-medium width. It is nicely seen that, at least for heavy nuclei like ^{197}Au , there are measurable changes in the absolute cross sections for $\Lambda(1520)$ production on these nuclei due to its in-medium width.

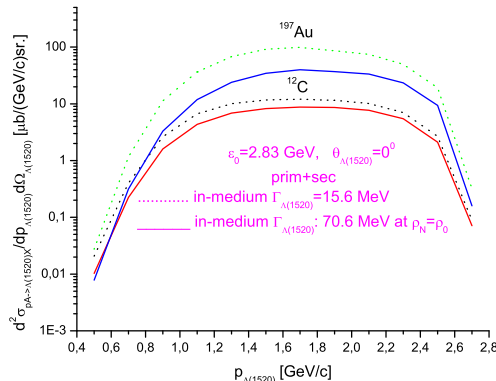


Figure 7: Double differential cross sections for the production of $\Lambda(1520)$ hyperons at an angle of 0° in the interaction of protons of energy 2.83 GeV with ^{12}C (two lower lines) and ^{197}Au (two upper lines) target nuclei as functions of $\Lambda(1520)$ momentum for the one- plus two-step $\Lambda(1520)$ creation mechanisms calculated within the different scenarios for the $\Lambda(1520)$ in-medium width. The dotted lines are calculations for the free $\Lambda(1520)$ width. The solid lines are calculations with employing for the $\Lambda(1520)$ in-medium width that shown by solid curve in figure 4.

We, therefore, come to the conclusion that the in-medium properties of the $\Lambda(1520)$ should be in principle observable through the target mass dependence of the absolute $\Lambda(1520)$ production cross section in pA reactions at above threshold beam energies.

However, the authors of ref. [20] have suggested to use as a measure for the $\Lambda(1520)$ width in nuclei the following relative observable—the double ratio: $R(A)/R(^{12}\text{C}) = (\sigma_{pA}/A)/(\sigma_{p^{12}\text{C}}/12)$, i.e. the ratio of the nuclear total $\Lambda(1520)$ production cross section from pA reactions divided by A to the same quantity on ^{12}C . But instead of this ratio, we consider the following analogous ratio $R(A)/R(^{12}\text{C}) = (\tilde{\sigma}_{pA}(p_{\Lambda(1520)}, 0^\circ)/A)/(\tilde{\sigma}_{p^{12}\text{C}}(p_{\Lambda(1520)}, 0^\circ)/12)$, where $\tilde{\sigma}_{pA}(p_{\Lambda(1520)}, 0^\circ)$ is the double differential cross section for the production of $\Lambda(1520)$ hyperons with momentum $p_{\Lambda(1520)}$ at a lab angle of 0° in proton–nucleus collisions.

Figure 8 shows the ratio $R(A)/R(^{12}\text{C}) = (\tilde{\sigma}_{pA}(p_{\Lambda(1520)}, 0^\circ)/A)/(\tilde{\sigma}_{p^{12}\text{C}}(p_{\Lambda(1520)}, 0^\circ)/12)$ as a function of the nuclear mass number A calculated on the basis of equations (4), (30) for the one-step and one- plus two-step $\Lambda(1520)$ creation mechanisms (corresponding lines with symbols 'prim' and 'prim+sec' by them) for the projectile energy of 2.83 GeV as well as for the $\Lambda(1520)$ momenta of 2.3 GeV/c, 1.7 GeV/c, 1.1 GeV/c and within the considered two scenarios for the $\Lambda(1520)$ in-medium width: (i) free $\Lambda(1520)$ width (dotted lines), (ii) in-medium $\Lambda(1520)$ width shown by solid curve in figure 4 (solid lines). Looking at this figure, one can see that there are visible experimentally separated differences between the results obtained by using different $\Lambda(1520)$ in-medium widths under consideration and the same assumptions concerning the $\Lambda(1520)$ production mechanism (between corresponding dotted and solid lines). The secondary pion-induced reaction channel $\pi N \rightarrow K\Lambda(1520)$ plays a minor role for all considered target nuclei at $\Lambda(1520)$ momentum of 2.3

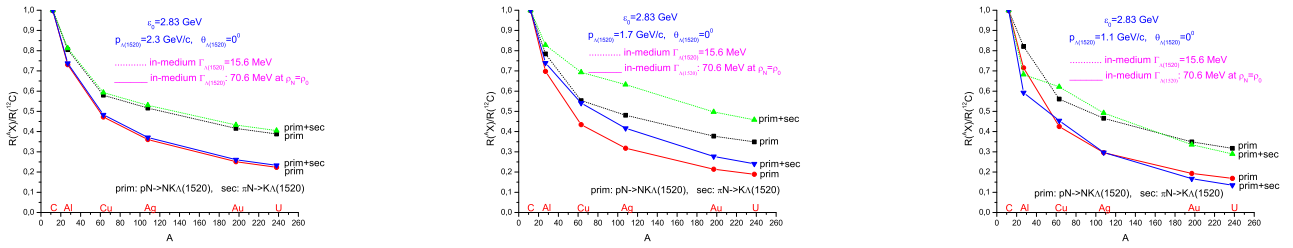


Figure 8: Ratio $R(A,X)/R(^{12}\text{C}) = (\tilde{\sigma}_{pA}(p_{\Lambda(1520)}, 0^\circ)/A)/(\tilde{\sigma}_{p^{12}\text{C}}(p_{\Lambda(1520)}, 0^\circ)/12)$ as a function of the nuclear mass number for initial energy of 2.83 GeV and for the $\Lambda(1520)$ momenta of 2.3 GeV/c (left panel), 1.7 GeV/c (middle panel), 1.1 GeV/c (right panel) calculated within the different scenarios for the $\Lambda(1520)$ hyperon production mechanism and for its in-medium width. For notation see the text.

GeV/c¹³. Although this channel contributes dominantly to the absolute $\Lambda(1520)$ creation cross section at $\Lambda(1520)$ momentum of 1.1 GeV/c (see figures 5, 6), it manifests themselves insignificantly at this momentum in the relative observable of interest for targets heavier than the Al target. This is due to the fact that at $\Lambda(1520)$ momentum of 1.1 GeV/c the two-step to one-step $\Lambda(1520)$ production cross section ratio for pA collisions is approximately equal to that for pC interactions. On the other hand, at $\Lambda(1520)$ momentum of 1.7 GeV/c there are clear differences between calculations corresponding to different suppositions about the $\Lambda(1520)$ creation mechanism and the same $\Lambda(1520)$ widths in the medium (between dotted lines, and between solid lines in the middle panel of figure 8). We may see, for example, that at this momentum for heavy nuclei the calculated ratio $R(A,X)/R(^{12}\text{C})$ can be of the order of 0.19 for the direct $\Lambda(1520)$ production mechanism and 0.24 for the direct plus two-step $\Lambda(1520)$ creation mechanisms in the case when the absorption of $\Lambda(1520)$ hyperons in nuclear matter was determined by their in-medium width shown by solid curve in figure 4. Since the main contribution to the nuclear total $\Lambda(1520)$ production cross section from direct mechanism comes, as figure 6 shows, from the $\Lambda(1520)$ momenta ~ 2.1 – 2.3 GeV/c as well as from small $\Lambda(1520)$ production angles due to the kinematics, we can compare to a first approximation the above ratio calculated with this width for the one-step $\Lambda(1520)$ creation mechanism at momentum of 2.3 GeV/c with the corresponding ratio of the nuclear cross sections obtained in [20] at beam energy of 2.9 GeV¹⁴ and for the nominal $\Lambda(1520)$ momentum-dependent in-medium width. By looking at the solid line with symbol 'prim' by it in the left panel of figure 8 and at the solid curve in figure 5 (top panel) from [20], we obtain that our results exceed the findings of [20] by factors of ≈ 1.1 , 1.2 and 1.5 for target nuclei Al, Cu and U, respectively. Such difference in the A dependences for the R ratios might be attributed in particular to the use in [20] the momentum-dependent $\Lambda(1520)$ in-medium width.

Thus, we can conclude that the high precision observation of the A dependence, like that considered above, can serve as an important tool to determine the $\Lambda(1520)$ width in nuclei and in the analysis of the observed dependence it is needed to account for in general the secondary pion-induced $\Lambda(1520)$ production processes. To put more strong constraints on this width one needs to compare the results of more reliable model calculations, based only on the direct $\Lambda(1520)$ production mechanism, with the respective high-momentum data.

Finally, in figure 9 we show together the results of our calculations, given before separately in figure 8, for the A dependence of our interest for the primary (1)–(3) plus secondary (29) $\Lambda(1520)$ production processes obtained for bombarding energy of 2.83 GeV by employing in them both the free $\Lambda(1520)$ hyperons width (dotted lines) and their in-medium width shown by solid curve in

¹³Which is in line with our findings of figures 5, 6.

¹⁴Which is close to that of the present work.

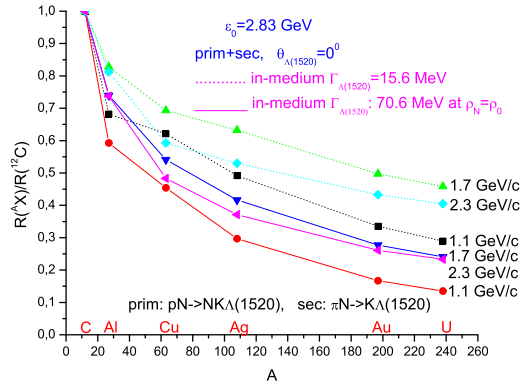


Figure 9: Ratio $R(A)/R(^{12}\text{C}) = (\tilde{\sigma}_{pA}(p_{\Lambda(1520)}, 0^\circ)/A)/(\tilde{\sigma}_{p^{12}\text{C}}(p_{\Lambda(1520)}, 0^\circ)/12)$ as a function of the nuclear mass number for the one- plus two-step $\Lambda(1520)$ production mechanisms calculated for incident energy of 2.83 GeV within the different scenarios for the $\Lambda(1520)$ in-medium width and for the choice of the $\Lambda(1520)$ momentum. For notation see the text.

figure 4 (solid lines) as well as the considered options ¹⁵ for the $\Lambda(1520)$ momentum to see also the sensitivity of the calculated A dependence to the $\Lambda(1520)$ momentum. One can see that the differences between the calculations for the same $\Lambda(1520)$ width shown by solid curve in figure 4 with adopting for the $\Lambda(1520)$ momentum two options: $p_{\Lambda(1520)} = 1.7$ GeV/c and $p_{\Lambda(1520)} = 2.3$ GeV/c (between two upper solid curves) are insignificant, which means that this relative observable depends weakly on the $\Lambda(1520)$ momentum in the high-momentum region 1.7 GeV/c $\leq p_{\Lambda(1520)} \leq 2.3$ GeV/c, where the cross section for $\Lambda(1520)$ production is larger. The measurement of such weak dependence should, in particular, reflect the fact that the $\Lambda(1520)$ width in the medium is momentum independent.

Thus, our results demonstrate that the measurements of the A and momentum dependences of the absolute and relative cross sections for $\Lambda(1520)$ production in pA reactions in the considered kinematics and at above threshold beam energies will allow indeed to shed light on its in-medium properties. They show also that to extract the definite information on the $\Lambda(1520)$ width in nuclear matter from the analysis of the measured such dependences it is needed to take into account in this analysis the secondary pion-induced $\Lambda(1520)$ production processes.

4. Conclusions

In this paper we have calculated the A and momentum dependences of the absolute and relative cross sections for $\Lambda(1520)$ production at a lab angle of 0° from pA reactions at 2.83 GeV beam energy by considering incoherent primary proton–nucleon and secondary pion–nucleon $\Lambda(1520)$ production processes in the framework of a nuclear spectral function approach [14, 15], which takes properly into account the struck target nucleon momentum and removal energy distribution, calculated using the one-pion-exchange model elementary cross sections for proton–nucleon reaction channel as well as two different scenarios for the total $\Lambda(1520)$ width in the medium. It was found that the secondary pion-induced reaction channel $\pi N \rightarrow K\Lambda(1520)$ contributes distinctly to the low-momentum $\Lambda(1520)$ production in the chosen kinematics and, hence, it has to be taken into consideration on close examination of these dependences with the aim to get information on the $\Lambda(1520)$ width in the nuclear matter. It was also shown that both the A dependence of the relative

¹⁵Indicated by the respective symbols by the lines.

$\Lambda(1520)$ hyperon production cross section and momentum dependence of the absolute $\Lambda(1520)$ hyperon yield from pA collisions in the considered kinematics and at incident energy of interest are appreciably sensitive to its in-medium width. This gives an opportunity to determine the $\Lambda(1520)$ width in the nuclear medium at finite baryon densities experimentally.

Acknowledgments

The author gratefully acknowledges M. Hartmann, Yu. Kiselev, V. Koptev, H. Ströher for their interest in the work. This work is partly supported by the Russian Fund for Basic Research, Grant No.07-02-91565.

References

- [1] R. Rapp and J. Wambach, *Adv. Nucl. Phys.* **25**, 1 (2000);
R. S. Hayano and T. Hatsuda, *nucl-ex/0812.1702*;
S. Leupold, V. Metag, U. Mosel, *nucl-th/0907.2388*.
- [2] M. M. Kaskulov and E. Oset, *AIP Conf. Proc.* 842: 483–485 (2006) [*arXiv:nucl-th/0512108*].
- [3] M. M. Kaskulov and E. Oset, *Phys. Rev. C* **73**, 045213 (2006).
- [4] T. Hatsuda and S. H. Lee, *Phys. Rev. C* **46**, R34 (1992).
- [5] F. Klingl, T. Waas, W. Weise, *Phys. Lett. B* **431**, 254 (1998).
- [6] E. Oset and A. Ramos, *Nucl. Phys. A* **679**, 616 (2001).
- [7] D. Cabrera and M. J. Vicente Vacas, *Phys. Rev. C* **67**, 045203 (2003).
- [8] V. K. Magas, L. Roca, E. Oset, *Phys. Rev. C* **71**, 065202 (2005).
- [9] D. Cabrera *et al.*, *Nucl. Phys. A* **733**, 130 (2004).
- [10] P. Muehlich and U. Mosel, *Nucl. Phys. A* **765**, 188 (2006).
- [11] T. Ishikawa *et al.*, *Phys. Lett. B* **608**, 215 (2005).
- [12] A. Sibirtsev, H.-W. Hammer, U.-G. Meissner, *Eur. Phys. J. A* **37**, 287 (2008).
- [13] A. Sibirtsev *et al.*, *Eur. Phys. J. A* **29**, 209 (2006).
- [14] E. Ya. Paryev, *Yad. Fiz.* **71**, 1985 (2008).
- [15] E. Ya. Paryev, *J. Phys. G.* **36**, 015103 (2009).
- [16] P. Muehlich and U. Mosel, *Nucl. Phys. A* **773**, 156 (2006).
- [17] M. Kaskulov, E. Hernandez, E. Oset, *Eur. Phys. J. A* **31**, 245 (2007).
- [18] E. Oset, M. Kaskulov, H. Nagahiro, E. Hernandez, and S. Hirenzaki, *nucl-th/0710.3033*;
- [19] M. Kotulla *et al.*, *Phys. Rev. Lett.* **100**, 192302 (2008).
- [20] M. Kaskulov, L. Roca, E. Oset, *Eur. Phys. J. A* **28**, 139 (2006).

- [21] M. Hartmann, Yu. Kiselev, *et al.*, ANKE–COSY proposal #147 (2005).
- [22] C. H. Lee *et al.*, Phys. Lett. B **412**, 235 (1997).
- [23] Z. Rudy *et al.*, Eur. Phys. J. A **15**, 303 (2002).
- [24] Z. Rudy *et al.*, Eur. Phys. J. A **23**, 379 (2005); erratum idid A **24**, 159 (2005) [arXiv:nucl-th/0411009].
- [25] M. L. Benabderrahmane *et al.*, Phys. Rev. Lett. **102**, 182501 (2009) [arXiv:nucl-ex/0807.3361].
- [26] E. Ya. Paryev, Eur. Phys. J. A **23**, 453 (2005).
- [27] O. Benhar, nucl-th/0307061.
- [28] Y. Nara, A. Ohnishi, T. Harada, A. Engel, Nucl. Phys. A **614**, 433 (1997).
- [29] V. Flaminio *et al.*, Compilation of cross sections. III: p and \bar{p} induced reactions. CERN-HERA **79 – 03** (1979).
- [30] T. Yao, Phys. Rev. **125**, 1048 (1962).
- [31] C. M. Ko, Phys. Rev. C **29**, 2169 (1984).
- [32] A. Sibirtsev, Nucl. Phys. A **604**, 455 (1996).
- [33] V. Flaminio *et al.*, Compilation of cross sections. I: π^- and π^+ induced reactions. CERN-HERA **79 – 01** (1979).
- [34] Y. Maeda *et al.*, Phys. Rev. C **77**, 015204 (2008).
- [35] S. V. Efremov and E. Ya. Paryev, Eur. Phys. J. A **1**, 99 (1998).
- [36] E. Ya. Paryev, Eur. Phys. J. A **7**, 127 (2000).
- [37] E. Ya. Paryev, Eur. Phys. J. A **9**, 521 (2000).
- [38] E. Ya. Paryev, Eur. Phys. J. A **17**, 145 (2003).